



Field Observations of Perforation Inflow Diagnostic (PID) Testing of Shallow Low-Permeability Gas Wells.

R.V. HAWKES

BJ Services Company Canada

H. DAKHLIA

BJ Services Company Canada

This paper is to be presented at the Petroleum Society's 5th Canadian International Petroleum Conference (55th Annual Technical Meeting), Calgary, Alberta, Canada, June 8 – 10, 2004. Discussion of this paper is invited and may be presented at the meeting if filed in writing with the technical program chairman prior to the conclusion of the meeting. This paper and any discussion filed will be considered for publication in Petroleum Society journals. Publication rights are reserved. This is a pre-print and subject to correction.

Abstract

In this paper, we present case studies of closed chamber testing of low-permeability gas wells immediately after perforating and observations made from interpretation of these tests. We refer to this type of testing as Perforation Inflow Diagnostic (PID) testing.

The procedure for PID testing is: 1) to remove liquids and gases from the wellbore in order to create maximum underbalanced conditions before perforating, and 2) to record surface and/or subsurface pressures in a closed chamber environment continuously throughout the fill up period of the wellbore.

The analysis process is to derive simultaneous gas inflow rate immediately after perforating using the closed chamber method to determine PID absolute open flow potential (AOF), in-situ gas permeability, wellbore skin and reservoir pressure. The assumptions of the diagnostic technique include isothermal and homogeneous reservoir conditions, single phase gas inflow, and constant gas chamber volume.

A majority of the cases where we applied this procedure show a well-behaved laminar inflow profile. However, a number of pressure responses show deviation from this idealized trend suggesting possible inflow of drilling mud filtrates or connate water inflow associated with the gas. In this paper, we present the well publicized backpressure plot as a diagnostic plot to help identify liquid inflow when only the simplest of surface recorders are utilized for field data measurements.

Introduction

Perforation Inflow Diagnostic (PID) tests, Impulse tests, Slug tests and Closed Chamber tests are all similar in methodology. By whatever name, they can provide estimates of maximum inflow (AOF) capability, flow capacity (kh), wellbore skin factor (S) and initial reservoir pressure (p_i).

The perforation inflow diagnostic (PID) testing analysis method is an extension (and specialization) of the closed chamber drillstem testing methods developed primarily in the

1970's by Lloyd Alexander¹. Field examples of this method in tight gas reservoirs together with typical diagnostic surface pressure plots were presented by Reid² in 1981. The method of closed chamber testing has proven to be a very effective procedure when applied to PID testing. The method is specifically applied to gas wells and is used to analyze the period subsequently after perforating a zone of interest³. Since the wellhead is shut in during the test, this procedure presents itself as a safe, cost effective, and environmentally friendly technique that can be performed using surface pressure recorders.

The purpose of this paper is to address the question "Does the pressure response subsequent to perforating provide meaningful reservoir information?"

The method involves using standard perforating equipment and operations. The technology involves conditioning the wellbore for maximum underbalanced perforating conditions and then monitoring the surface and/or subsurface pressure response. Unlike conventional testing procedures, the surface valve is closed during the entire flow period and the formation fluids are produced into the closed chamber (casing and or tubing volume). The pressure response measured after perforating is converted to gas inflow rates using established closed chamber calculations. This pressure and rate data can then be applied to transient flow theory for well and reservoir evaluations.

Closed Chamber Theory

This method is particularly concerned with measuring the so-called "afterflow" pressures after perforating the well. The flow is referred to as "afterflow" because the gas in the well chamber is flowing during the impulse period since perforating the well. Figure 1 is an example of both the pressure (left hand y axis) and inflow gas rate (right hand y axis) response from a typical PID test. The resistance to inflow (exerted by the gas that already occupies the wellbore chamber) is accounted for by the changing gas compressibility and the volume of the gas in the chamber. As illustrated in Figure 1, the ever increasing wellbore pressure increases as the reservoir continues to flow (in accordance with Darcy's law) against an increasing backpressure exerted by the well as reservoir gas invades the wellbore chamber.

Closed chamber theory states that we first start with the material balance equation,

$$q_{in} = q_{out} - \frac{dV}{dt} \dots\dots\dots (1)$$

that states that the fluid entering the "control volume" V (our wellbore chamber) from the reservoir (q_{in}) is equal to the amount of fluid produced at surface (q_{out}) minus a change in the volume of the gas due to changes in the chamber conditions (dV/dt). The definition of the isothermal compressibility of an ideal gas is,

$$c_w = -\frac{1}{V} \left(\frac{\partial V}{\partial p} \right) \dots\dots\dots (2)$$

The subscript "w" signifies the wellbore chamber. The isothermal condition is assumed to be the average chamber temperature. Using the chain rule of calculus we obtain the equation,

$$q_w = V_w c_w \frac{d p_w}{dt} \dots\dots\dots (3)$$

q_w is the flow rate in the wellbore chamber caused by the changing compressibility of the gas and the driving pressure gradient at average conditions. The product of $V_w c_w$ constitutes the so-called wellbore storage constant. Equation 3 then becomes the working equation for determining gas inflow rates during closed chamber conditions.

The combination of *maximum* underbalanced perforating conditions, the ability to monitor accurate surface pressures at high sampling rates (1 second), and the simultaneous closed chamber gas rates provide the ability to observe a high number of data and their relationship, particularly at very early times during underbalanced perforating. Useful well performance information such as perforation cleanup can be easily detected.

Transient Flow

Proper analysis of the pressure buildup response during perforation inflow testing requires that both pressure and rate be defined at certain conditions in order for an equating relationship to be developed. This is particularly true for gas since it has widely varying properties with changing pressure.

We can equate this change in wellbore volume of the gas through Darcy's equation yielding,

$$q_{in} = q_w = -\frac{kh}{\mu} \frac{\partial p}{\partial r} \dots\dots\dots (4)$$

During surge, impulse or perforation inflow tests, both pressure and flow rate are changing with time. Conventional pressure transient analyses methods require a constant rate (or constant pressure) solution in order for an analysis to be carried out. Meunier, Wittman and Stewart⁴ developed an equation for the infinite-acting radial flow equation for transient analysis based on Duhamel's principle (first applied by van Everdingen and Hurst⁵) to "normalize" pressure for variations in flow rate. This is essential in the analysis of afterflow data. Their equation is,

$$p_{wD}(t_D) = \int_0^{t_D} \frac{\partial q_D(\tau)}{\partial \tau} p_D(t_D - \tau) d\tau + q_D(t_D) S \dots\dots\dots (5)$$

where t_D is dimensionless time, p_D is the constant rate solution of the flow model, q_D is dimensionless flow rate, and S is skin factor.

The selected flow model is that of radial cylindrical flow in a homogeneous, infinite reservoir. The logarithm approximation to the solution at the wellbore is:

$$p_D(t_D) = \frac{1}{2} [\ln(t_D) + 0.80907] + S \dots\dots\dots (6)$$

Based on the work of Simmons⁶ and Tariq⁷, and using normalized pseudo-pressure⁸, the working equation for gas then becomes,

$$p_{(pm)i} - p_{(pm)w} = \tilde{m} \left[\log_{10}(t) + \frac{\Sigma_0}{q_{ref}} + \frac{q(t)}{q_{ref}} S \right] \dots\dots\dots (7)$$

where,

$$\begin{aligned} \Sigma_0 = & \\ & \sum_{j=1}^{n-1} \left[\left(\frac{q_{j+1} - q_j}{t_{j+1} - t_j} \right) \left((t_n - t_j) \log_{10}(t_n - t_j) - (t_n - t_{j+1}) \log_{10}(t_n - t_{j+1}) \right) \right] \quad (8) \\ & + \dots + 0.434(q_{ref} - q_n) + (q_n - q_{n-1}) \log_{10}(q_n - q_{n-1}) \end{aligned}$$

and,

$$\tilde{m} = \alpha \frac{q_w \left(\frac{Z_R p_w}{Z_w Z_R} \right) \mu_R}{kh} \dots \dots \dots (9)$$

Where α is a conversion factor. The right hand side of Equation 7 is plotted as the x axis and the left side of the equation as the y axis. The value of $p_{(pn)r} - p_{(pn)w}$ being the "closed-in" chamber pressure and the slope of the term (referred to as the rate convolved time) can be solved for \tilde{m} .

Application of the rate convolution method as presented in Equation 7 will, by definition, reduce the entire data set to a single linear trend. This is accomplished by discretizing the continually varying flow rates that occur during the closed chamber perforation inflow test. Practically speaking however, the early time period immediately after perforating the well will ordinarily be the time during which the instantaneous "spurt" production occurs due to the perforation process as well as perforation cleanup and will typically look like data scatter.

As Equation 7 illustrates, the knowledge of skin (S) is required before the pressure data can be plotted. Therefore, an initial estimate of kh is derived by initially assuming a starting value for skin (typically 0 to +5.0). Figure 5 is an example of a rate convolved time plot showing three curves representing three (3) different assumed skin values. Because of the continual decrease in flow rates during the chamber fill-up, time progresses to the left. Additionally, as the rate decays with time, the pressure curves converge to form a common straight line, regardless of the assumed skin value. Determination of kh is then inversely proportional to the slope of the curve (Equation 7).

Case Studies

In the rest of this paper, we present 3 field examples to illustrate the interpretation methodology and clearly show the application of the technology on low permeability gas wells. First we demonstrate the applicability of the individual steps of the interpretation showing flow regime identification and the introduction of the backpressure log-log plot for single phase gas, laminar inflow identification. Field example 2 demonstrates the application of the backpressure plot to identify deviation from the idealized inflow response suggesting inflow of drilling mud filtrates and/or connate water associated with gas inflow. Field example 3 is presented to further demonstrate the application of the technology on multi-zone perforations for inflow distribution identification.

Field Example 1

In this field example, we show the flow regime identification procedure, reservoir pressure extrapolation method, and identification of single phase laminar gas inflow. We also present the application of the closed chamber gas rate convolution method for determination of reservoir flow capacity (kh) and wellbore skin (S). A post frac production history on the well clearly shows the application of the technique as a pre

frac testing procedure for post frac prediction, an important tool for any hydraulic fracturing optimization program.

The example well is an Ellerslie formation which is a mid-Cretaceous sandstone in central Alberta. The zone of interest was perforated with wireline guns from 1265.0–1269.5 m (17 spm) in 114.3 mm casing with a cushion depth below the perforated interval at 1280 m. Surface recorders were installed and the surface pressures were measured for approximately 16 h. An acoustic well sounder shot was taken the next day to verify a dry wellbore condition for surface to subsurface calculations. Figure 1 illustrates the pressure and the closed chamber gas rate response during the 16 h PID test. Due to the dp/dt relationship of the gas inflow rate calculation there can be some scatter in the data in early times as shown on Figure 1. It is good practice after perforating to have the perforation guns sit on bottom for 60 minutes to allow a clean signal to be measured by the recorders prior to retrieving the guns out of the well.

Kuchuk⁹ presented a new method for determination of reservoir pressure. The technique is based on the wellbore pressure solutions to an instantaneous source, including wellbore storage (afterflow). The method introduced by Kuchuk uses the time function of $1/\Delta t_a$ (inverse pseudo-time for gas). Figure 2 is the Inverse Time plot from field example 1 showing a development of a straight line at around 3 h after perforating the well. Extrapolation of the curve to $1/\Delta t_a=0$ yields a reservoir pressure of 3431 kPa at mid-point perforation depth. The rate of pressure change in Figure 2 from 3 h to the end of the test is 7.6 kPa/h. The "rule of thumb" of 2 kPa/h is an excellent rule and can be used by field personnel to estimate the end of buildup for most PID tests.

Figure 3 shows a derivative plot of the calculated subsurface pseudo pressure vs. delta-pseudo-time. Unlike conventional well testing when equivalent time is used to account for the previous flow time, delta time is used for flow regime identification for PID tests. The -1 slope therefore is used to identify the "end of afterflow" and the start of reservoir transient (radial) flow. Note the start of a well-developed slope of -1 is also at 3 h supporting the straight line extrapolation on the Inverse Time plot (Figure 2).

One of the more significant diagnostic plots that this paper addresses is the widely used gas deliverability or AOF backpressure plot (Δp^2 versus gas inflow rate). Once reservoir pressure is determined, then pressure and rate data can be plotted on a conventional deliverability log-log plot to determine the wells instantaneous AOF potential. Shown as Figure 4 is a graph of Δp^2 versus q_{sc} from the data set of Example 1. Although pseudo pressure is traditionally the preferred method for handling gas flow equations, we propose the use of the pressure squared method because it is readily applied in the field.

As Figure 4 illustrates, the initial inflow character of the well follows a straight line reciprocal slope (n) of 1.0 indicating single phase laminar inflow. This relationship therefore provides the means to determine the PID AOF of the well of $7.45 \cdot 10^3 \text{ m}^3/\text{d}$ immediately after perforating. Upon careful inspection of Figure 4 we see that once backpressure increases and more importantly transient flow dominates the inflow, the curve transitions off the reciprocal straight line. To apply this technique effectively, the wellbore requires extreme underbalanced conditions, typically 80% of the estimated reservoir pressure.

Although the AOF value from a PID test does not describe a well's long-term deliverability, Leech, Hawkes, Storey, and Brown³ showed a useful predictive relationship between PID AOFs and post frac 30-day production results.

Figure 5 is a plot of normalized pseudo-pressure versus the closed chamber rate convolution time function. A skin value of

+3 yields the best straight line resulting in a $kh = 7.5$ mD.m. Typically, in identifying the best straight line, one starts out by choosing an approximate value of skin and making a plot. In most cases, only a few iterations are necessary to converge on the correct skin, making for the proper identification of the slope of the straight line for calculation of kh . Using commercially available gas simulators, a production forecast can be generated to evaluate the completion enhancement necessary for final production requirements.

In this field example, the results of the PID test were used to design a 20-tonne nitrified-foam, hydraulic fracture treatment and a subsequent tie-in for production. Figure 6 is the 90 day post frac production history on the well. The post frac production behaviour of the well compares very well with what was expected from the PID test results. It is worth noting that as observed by Leech, Hawkes, Storey, and Brown³, the relationship between a well's PID AOF and the initial production rate post frac usually works when the PID skin is low and most of the pay zone is exposed when perforating the well.

Field Example 2

Our second example is a shallow gas Bow Island interval in south east Alberta. The well was perforated between 692.0 – 693.0m with a 16 gram shallow gas gun at a density of 13 spm. Well log analysis indicated a 1 m high porosity streak of 22%. Potential filtrate invasion is also identified from medium and deep induction log responses. The objective of the PID test was to evaluate the interval for tie-in consideration and a possible stimulation candidate.

Pressures were recorded every 3 seconds and simultaneous gas rates were determined using closed chamber calculations. Pressure and flow rate are presented on Figure 7. Our proposed diagnostic (backpressure) plot is shown as Figure 8. In this field example, the curve exhibits an S shape from the inflow PID response. This distinct character is believed to be the result of two-phase, water and gas, inflow. The S shape of the diagnostic plot shows that the gas rate inflow is reduced due relative permeability effects caused by high water saturation locally. Reid^{2,10} has observed a similar S shape response in Cartesian plots of shut-in buildup curves from drillstem tests. These suggest either 1) a single phase gas zone cleaning up (dp/dt is accelerating, thus the afterflow rate q is also increasing as the well is continuing to flow at increasing rates while shut in at the surface); or 2) two-phase flow: liquid and gas (either - solution gas and oil in a low kh or badly damaged oil zone, -or condensate and gas, -or water and gas, -or mud filtrate and gas in a gas zone). This occurs because of the following relationship for liquid flow into a gas filled closed chamber (Alexander¹):

$$\frac{dp}{dt} = \frac{p}{V} \frac{dV}{dt} \dots\dots\dots (10)$$

Work by McKinley^{11,12} shows a 2 to 5 fold increase in oil well productivity when using the computed liquid permeability from a DST when the mobile gas saturation in the wellbore region is between 10% and 20% respectively. By definition, the presence of a second phase in the near wellbore porous medium obstructs flow, alters the fluid flow mechanics in the pore space, and results in decreased flow capacity. Recent studies, performed by the Stim-Lab Proppant Consortium¹³, suggest that the magnitude of flow capacity of a sand pack in two-phase flow may be 20 times less than the flow capacity in single phase flow under the most adverse flow conditions.

Results derived from the PID test in field example 2 gave a PID-AOF of $0.7 \cdot 10^3$ m³/d and an unexpected low flow capacity (kh) value of 0.13 mD.m. The wellbore skin value was +1.5. The results of the analysis were surprising to the operator considering the relatively high porosity of the perforated interval. In consideration of the poor results, the well was re-perforated over a larger interval (691.0-694.0m) with larger guns and charges (86mm EHSC 25gSDP x 60deg). The well was tested again using surface recorders to measure the buildup response subsequent to re-perforation. As shown by Figure 9, the inflow response was stronger after re-perforating the well with larger charges. Additionally however, the surface pressures did not recover to the original surface pressure of 3575 kPa due to an influx of approximately 60 m of formation liquid produced into the wellbore. It was concluded that the liquid saturation of the zone was too high as a hydraulic fracturing candidate and uneconomical at the current conditions for tie-in.

Field Example 3

In this example we present a multi-zone perforating sequence on a Viking formation in central Alberta. The lower interval, 660.0–662.0 m, was initially perforated and surface pressure was monitored for 1.9 h. Since the wellbore pressure was close to static conditions prior to running in the hole with the second set of guns, the well was blown down again to achieve maximum underbalanced conditions. The well was blown down to approximately 80% of the expected reservoir pressure and upper Viking was perforated from 656.0 – 657.0 m. Figure 11 is a pressure plot showing both the pressure response of both the lower and upper Viking perforated intervals and the corresponding closed chamber gas rates. Upon careful inspection of Figure 11, there is no apparent increase in gas inflow. When the same data is plotted on the backpressure diagnostic plot (see Figure 12), we see clearly there was no flow contribution from the upper Viking interval.

Figure 13 is the Inverse Time plot of the pressure response after perforating the upper Viking zone. This plot demonstrates a late time reservoir heterogeneity response typical of reduction in permeability away from the wellbore. Since no measurable inflow was identified from the upper Viking zone, we can then conclude that the lower Viking zone is the interval demonstrating the heterogeneity. Figure 14 demonstrates the pressure derivative response of the same data set. Radial flow is identified well before an hour of perforating as illustrated by the -1 slope on the log-log plot. The pressure derivative response at 2.1 h is verified as a reservoir heterogeneity effect.

Limitations and Recommendations

Successful application of the Perforation Inflow Diagnostic technique is dependent upon proper conditioning of the wellbore to achieve maximum underbalanced perforating conditions and accurate surface (and/or subsurface) pressure and temperature recorders. Noisy pressure data can significantly influence the interpretation methodology. Presence of co-produced liquids can significantly affect gas inflow response resulting in S curves in log-log and linear plots of pressure data.

Conclusion

The assumptions made in deriving this method are a single homogenous layer, isothermal, dry gas flow. When those conditions are met, a closed chamber gas rate convolution time function and interpretation method is presented that allows meaningful reservoir and wellbore information from

the pressure response subsequent to underbalanced perforating. When there is a deviation in one of the assumptions, then we point out in this paper the interpretation methodology and how that can be detected in one of more of the presented diagnostic plots. When liquid is co-produced (filtrate, connate water, or condensate), we present the backpressure plot as a practical and useful diagnostic plot to identify deviation from idealized inflow profile. When there is multi-layer heterogeneity, the derivative diagnostic plot shows a sustained slope above the -1 slope.

Acknowledgement

The authors would like to thank BJ Services Company Canada for support and permission to write this paper.

NOMENCLATURE

AOF	=	Absolute Open Flow potential (gas)
c	=	compressibility
h	=	reservoir thickness
k	=	permeability
kh	=	flow capacity
\tilde{m}	=	slope on the PID plot
n	=	slope on the backpressure plot
p	=	pressure
PID	=	Perforation Inflow Diagnostic
q	=	gas rate
r	=	radius
S	=	skin factor
spm	=	shots per metre
t	=	time
V	=	volume
Z	=	real gas deviation factor
Δt_a	=	delta pseudo time

Greek Letters

α	=	conversion constant
μ	=	viscosity
Σ	=	sum operator
τ	=	integration variable

Subscripts

D	=	dimensionless
i	=	initial
in	=	inflow
j,n	=	indices
out	=	out flow
pn	=	normalized pseudo (pressure)
R	=	reservoir
ref	=	reference
sc	=	standard conditions
w	=	wellbore

REFERENCES

- Alexander, L.G., "Theory and Practice of the Closed Chamber Drillstem Test Method," *Journal of Petroleum Technology*, pp. 1539-1544, December 1977.
- Reid, H.W., "Evaluation of Low Permeability Gas Reservoirs Utilizing Closed Chamber Drillstem Test Techniques," *paper SPE 10184 prepared for presentation at the 56th SPE Annual Technical Conference and Exhibition, San Antonio, Texas, October 5-7, 1981.*
- Leech, D., Hawkes, R., Storey, P, Brown, S., "Impulse, Perforation, and Closed Chamber Testing: Simple, Quick, Cost-effective Snapshots of Reservoir Inflow Characteristics," *paper CIPC 2000-80 prepared for presentation at the Petroleum Society's Canadian International Petroleum Conference, Calgary, Alberta, June 4-8, 2000.*
- Meunier, D., Wittmann, M.J., and Stewart, G., "Interpretation of Pressure Buildup Test Using In-Situ Measurements of Afterflow," *Journal of Petroleum Technology*, pp. 143-152, January 1985.
- van Everdingen, A.F. and Hurst, W., "The Application of the Laplace Transformation to Flow Problems in Reservoirs," *Trans., AIME Vol. 186*, pp. 305-324, 1949.
- Simmons, J.F., "Interpretation of Underbalanced Surge Pressure Data by Rate-Time Convolution," *paper SPE 15477 prepared for presentation at the 61st SPE Annual Technical Conference and Exhibition, New Orleans, Louisiana, October 5-8, 1986.*
- Tariq, S.M., "Rate-Convolved Horner Plot for Analysis of simultaneously Acquired Flow Rate and Pressure Data," *paper SPE 19816 prepared for presentation at the 64th SPE Annual Technical Conference and Exhibition, San Antonio, Texas, October 8-11, 1989.*
- Meunier, D.F., Kabir C.S., Wittmann, M.J., "Gas Well Test Analysis: Use of Normalized Pseudovariables," *SPE Formation Evaluation, December 1987.*
- Kuchuk, F.J., "A New Method for Determination of Reservoir Pressure," *paper SPE 56418 prepared for presentation at the SPE Annual Technical Conference and Exhibition, Houston, Texas, October 3-6, 1999.*
- Reid, H.W., "Modern Concepts in Drillstem Testing of Use to the Geologist and Engineer," *Text accompanying workshop presented at the 1979 joint convention of the Canadian Society of Petroleum Geologists and Canadian Society of Exploration Geophysicists, Calgary, Alberta, June 10-13, 1979.*
- McKinley, R.M., "Wellbore Transmissibility from Afterflow-Dominated Pressure Buildup Data," *SPE Journal*, 1971.
- McKinley, R.M., "Estimating Flow Efficiency From Afterflow-Distorted Pressure Buildup Data," *SPE Journal*, pp. 696, 1974.
- Barree, R.D., "Multiphase Flow Corrections in Non-Darcy Flow Conditions," *prepared for presentation at the STIM-LAB Proppant Consortium Meeting, February 26-27, 2004.*

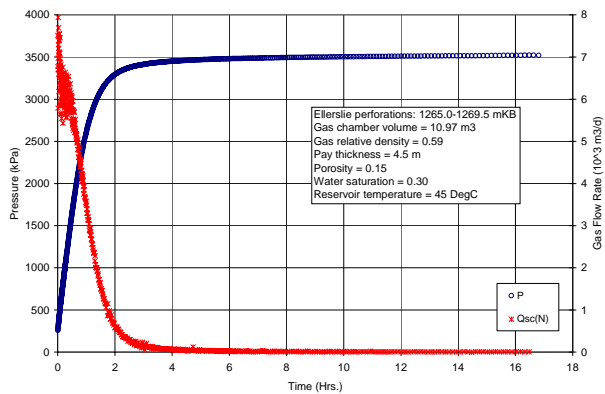


Figure 1. Closed chamber gas rate.

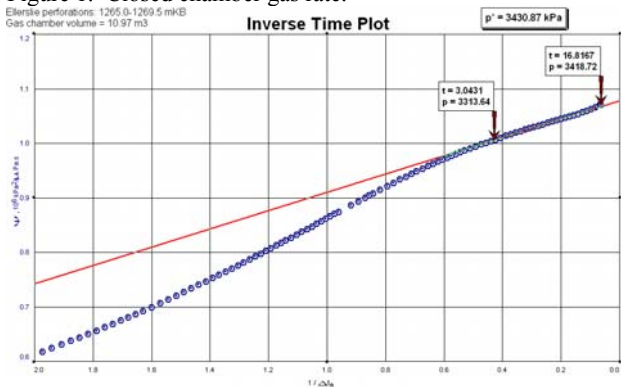


Figure 2. Inverse time plot for Example 1.

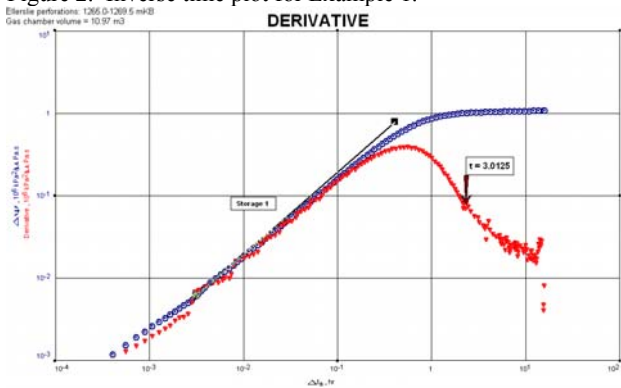


Figure 3. Pressure derivative diagnostic plot of Example 1.

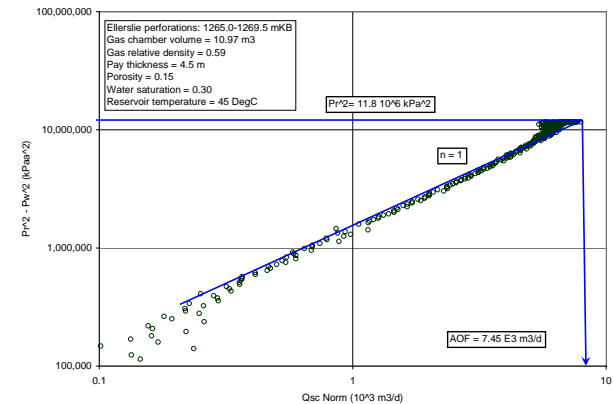


Figure 4. Backpressure plot of Example 1.

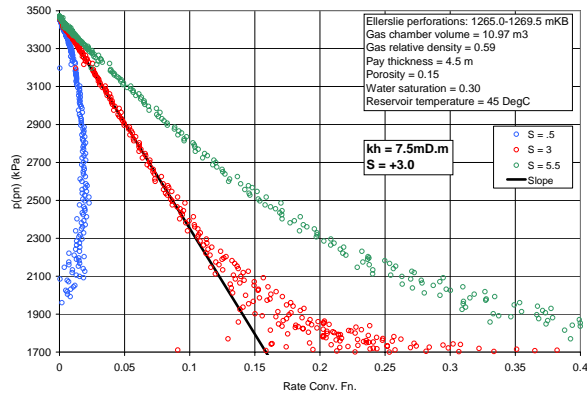


Figure 5. PID plot of Example 1.

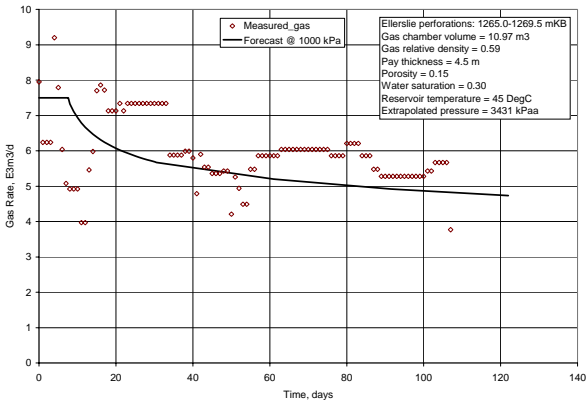


Figure 6. 90 day post frac production plot of Example 1.

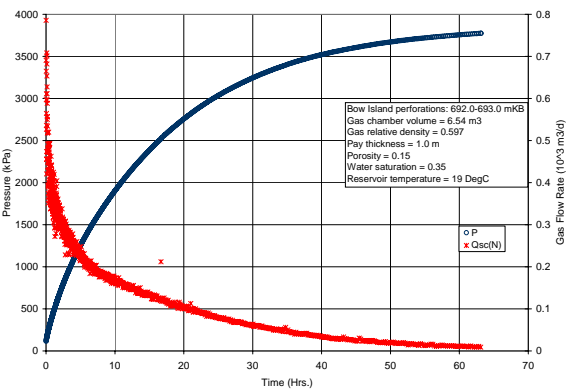


Figure 7. Calculated closed chamber gas rate of Example 2.

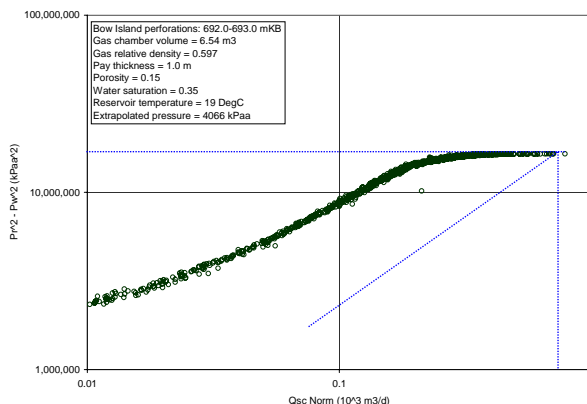


Figure 8. Backpressure diagnostic plot of Example 2.

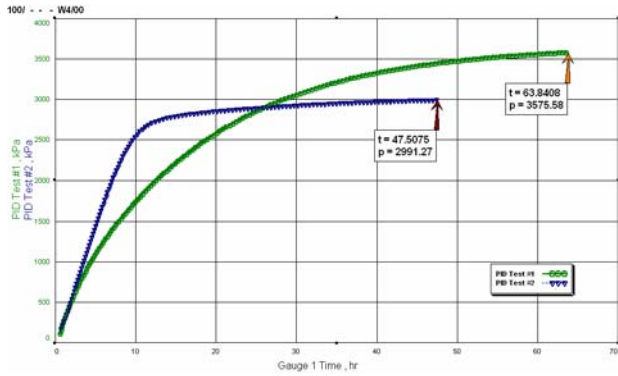


Figure 9. Overlay of original and second PID test pressure data.

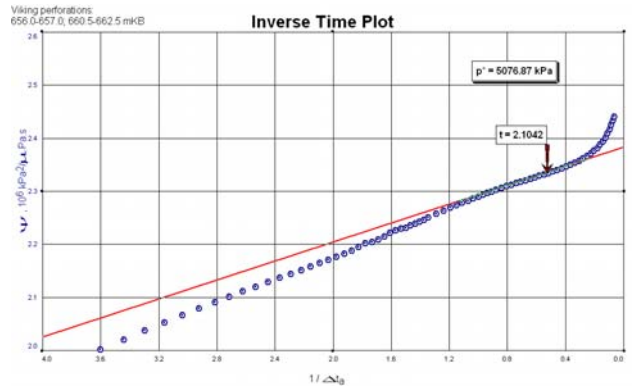


Figure 13. Inverse time plot for Example 3.

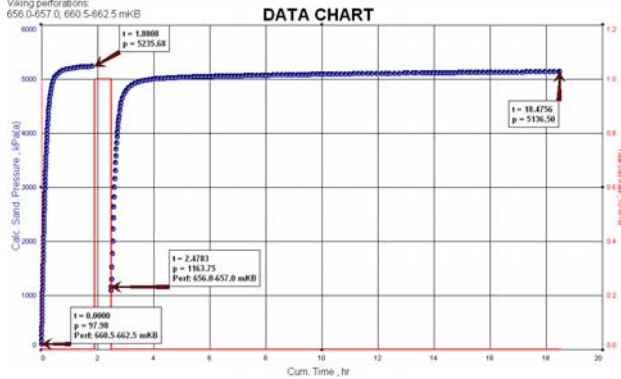


Figure 10. Pressure profile of Example 3.

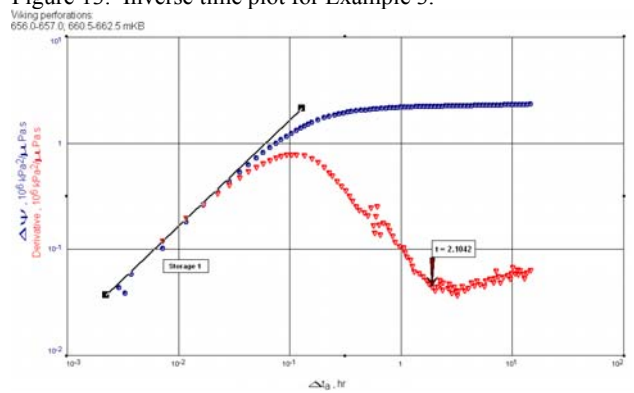


Figure 14. Pressure derivative plot of Example 3.

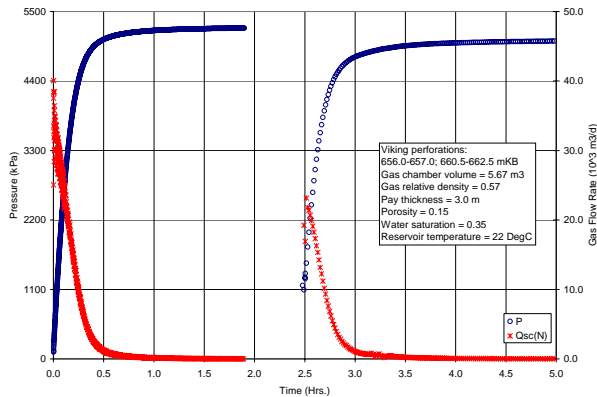


Figure 11. Pressure profile and closed chamber gas rate of Example 3.

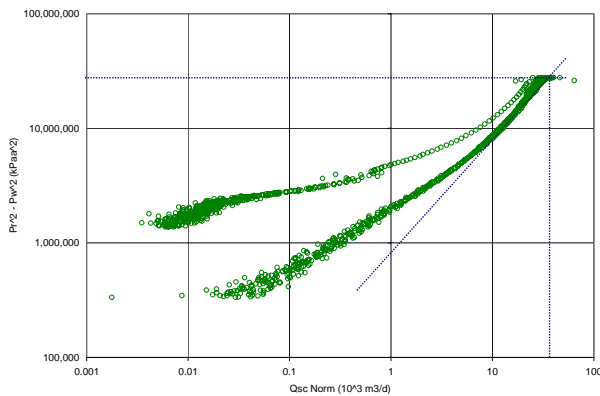


Figure 12. Backpressure diagnostic plot of Example 3.